Nicholas, Andrew P, Clarke, Lucy E ORCID: 0000-0002-8174-3839 and Quine, Timothy A (2009) A numerical modelling and experimental study of flow width dynamics on alluvial fans. Earth Surface Processes and Landforms, 34 (15). pp. 1985-1993. doi:10.1002/esp.1839

Official URL: http://onlinelibrary.wiley.com/doi/10.1002/esp.1839/abstract
DOI: http://dx.doi.org/10.1002/esp.1839
EPrint URI: https://eprints.glos.ac.uk/id/eprint/2957

EARTH SURFACE PROCESSES AND LANDFORMS
Earth Surf. Process. Landforms (2009)

Published online in Wiley InterScience
(www.interscience.wiley.com) DOI: 10.1002/esp.1839

A numerical modelling and experimental study flow of width dynamics on alluvial fans

A. P. Nicholas,* L. Clarke and T. A. Quine
School of Geography, University of Exeter, Exeter, UK

Received 30 June 2008; Revised 30 March 2009; Accepted 27 April 2009

* Correspondence to: A. P. Nicholas, School of Geography, University of Exeter, Exeter, EX4 4RJ, UK. E-mail: A.P.Nicholas@exeter.ac.uk

ESPL
Earth Surface Processes and Landforms

ABSTRACT: Alluvial fans are dynamic landforms, the evolution of which is controlled by both external environmental forcing (climate, tectonics and base level change) and internal process-form feedbacks. The latter include changes in flow configuration (between sheetflow and channelized flow states), driven by aggradation and degradation, which may in turn promote changes in sediment transport capacity. Recent numerical modelling indicates that such feedbacks may lead to dramatic and persistent fan entrenchment in the absence of external forcing. However, the parameterization of flow width within such models is untested to date and is subject to considerable uncertainty. This paper presents results from an experimental study of flow width dynamics on an aggrading fan in which spatial and temporal patterns of fan inundation are monitored continuously using analysis of digital vertical photography. Observed flow widths are compared with results from a simple theoretical model developed for non-equilibrium (aggradational) conditions. Results demonstrate that the theoretical model is capable of capturing the first-order characteristics of width adjustment over the course of the experiment, and indicate that flow width is a function of fan aggradation rate. This illustrates that models of alluvial flow width derived for equilibrium conditions may have limited utility in non-equilibrium situations, despite their widespread use to date. Copyright © 2009 John Wiley & Sons, Ltd.

KEYWORDS: alluvial fan; flow width; aggradation; physical experimentation; numerical model

Introduction

The relative importance of autogenic and allogenic controls on landscape evolution is a topic of ongoing debate in fluvial geomorphology and has received much recent attention (Francis, 2006; Muto and Swenson, 2006; Kim and Muto, 2007; Nicholas and Quine, 2007; Stouthamer and Berendsen, 2007; Kim and Jerolmack, 2008). However, in field settings, where records of past environmental change are fragmentory and understanding of geomorphic processes is incomplete, disentangling the effects of environmental forcing (e.g. climate, tectonics and base level change) from internally-driven process-form feedbacks is often problematic. Previous studies of alluvial fans have demonstrated that these landforms afford considerable potential to contribute to this debate, not least because their limited extent (length) may promote relatively rapid and complex response to both internal and external perturbations (Hooke and Dorn, 1992; Harvey, 2002a; Viseras *et al.*, 2003). Field-based interpretation of fan morphology and stratigraphy has often emphasized the role of external environmental forcing (Ritter *et al.*, 1995; Whipple and Trayler, 1996; Harvey, 2002b; Hartley *et al.*, 2005; Harvey, 2005). For example, Figure 1 shows a heavily entrenched tributary fan in the Avoca Valley, South Island, New Zealand, which could be interpreted to reflect a para-glacial decline in sediment supply (cf. Church and Ryder, 1972) and an associated drop in base level resulting from vertical or lateral erosion within the main valley floor to which the fan is coupled.

Figure 1. Entrenched tributary fan in the Avoca Valley, South Island, New Zealand. Fan length is *c.* 1·1 km. Fan apex elevations for extensive high early post-glacial surface and contemporary channel are *c.* 90 m and 40 m, respectively.

Numerical and physical modelling has shown that autogenic mechanisms may drive complex fluvial responses to external forcing (Schumm and Parker, 1973; Humphrey and Heller, 1995; Coulthard *et al.*, 2002), and promote short-term, localized erosion and sedimentation on fans (Schumm *et al.*, 1987; Whipple *et al.*, 1998). More recently, Nicholas and Quine (2007) have shown that internal dynamics associated with a transition from sheetflow dominated conditions to channelized flow might drive dramatic and persistent fan

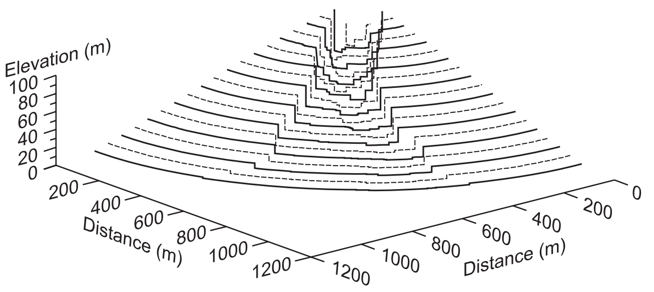

Figure 2. Alluvial fan morphology simulated by the numerical model of Nicholas and Quine (2007). In this 18 000 year simulation, a period of fan progradation and stabilization (at the level of the upper surface shown in this diagram) is followed by large-scale fan entrenchment that is a product of internally-driven feedbacks between fan size, aggradation rate, flow width and sediment transport capacity. Superimposed on this long-term degradational trend, short-term (decadal to centennial scale) fluctuations in water and sediment supply promote the formation of a complex sequence of unpaired terraces.

entrenchment as a natural consequence of declining aggradation rates associated with fan growth. Figure 2 shows results from a simulation of the case where tributary fan progradation is limited by coupling to a larger fluvial system in the main trunk valley. Declining aggradation rates result from increasing fan area during progradation and, following coupling to the main valley floor, lack of accommodation space. This in turn promotes a reduction in total flow width on the fan and an increase in sediment transport capacity that initiates incision, leading to the entrenchment seen in Figure 2. The resulting flow narrowing (channelization) and associated degradation is distinct (in both magnitude and longevity) from the short-term, small-scale cyclicity evident in past physical modelling studies (Schumm *et al.*, 1987; Whipple *et al.*, 1998) and might promote fan entrenchment in natural environments in the absence of either climatic or tectonic forcing. However, at present this possibility remains an untested hypothesis that hinges on dynamic changes in flow configuration during fan evolution, and more specifically in the model formulation presented by Nicholas and Quine (2007), on the relationship between active flow width and rate of fan aggradation. Unfortunately, understanding of the controls on the width and configuration of flow in rivers and on fans under non-equilibrium conditions remains incomplete. Consequently, existing quantitative models typically represent alluvial flow width using hydraulic geometry relationships (Clevis *et al.*, 2003), equilibrium theory (Parker *et al.*, 1998), or as a prescribed boundary condition (Kim and Jerolmack, 2008). Here we present preliminary results from an experimental study designed to quantify spatial and temporal changes in flow configuration during alluvial fan construction, and compare these data with the non-equilibrium flow width model of Nicholas and Quine (2007).

Theoretical Modelling of Flow Width on Alluvial Fans

Flow width is an important variable in any model of geomorphic processes, in part because it is a key control on sediment transport rate. Consequently, changes in flow width, due to aggradation or degradation, may promote feedbacks by either enhancing or suppressing sediment transport. Relatively little attention has been given to the problem of modelling (predicting) flow width on alluvial fans for either equilibrium or non-equilibrium conditions. Parker *et al.* (1998) present two alternative models for representing flow width on fans under conditions of equilibrium aggradation (where fan aggradation is balanced by basin subsidence). The first model applies to the case of sheetflow dominated fans and assumes that flow occupies a constant fraction of the fan as one moves downfan (referred to as the expanding sheetflow model). The second model applies to the case of channelized flow (for both single and multi-thread channel systems) and is based on the assumption that the dimensionless shear stress within the channel will equal a constant multiple (*c.* 1·4) of the critical dimensionless shear stress (Parker, 1978). This well known width closure model for alluvial channels is supported by considerable empirical evidence (cf. Parker *et al.*, 1998). When combined with appropriate equations representing mass continuity, flow resistance (e.g. a Manning–Strickler law) and sediment transport (e.g. a Meyer-Peter and Muller relation) it implies that flow width is proportional to sediment transport rate. In the case of fans experiencing equilibrium aggradation (defined earlier) this implies a reduction in flow width downfan driven by the declining sediment transport rate that results from upfan aggradation (Parker *et al.*, 1998). Typical relationships between fractional flow width (flow width divided by fan width) and distance downfan for these two models are shown in Figure 3(a).

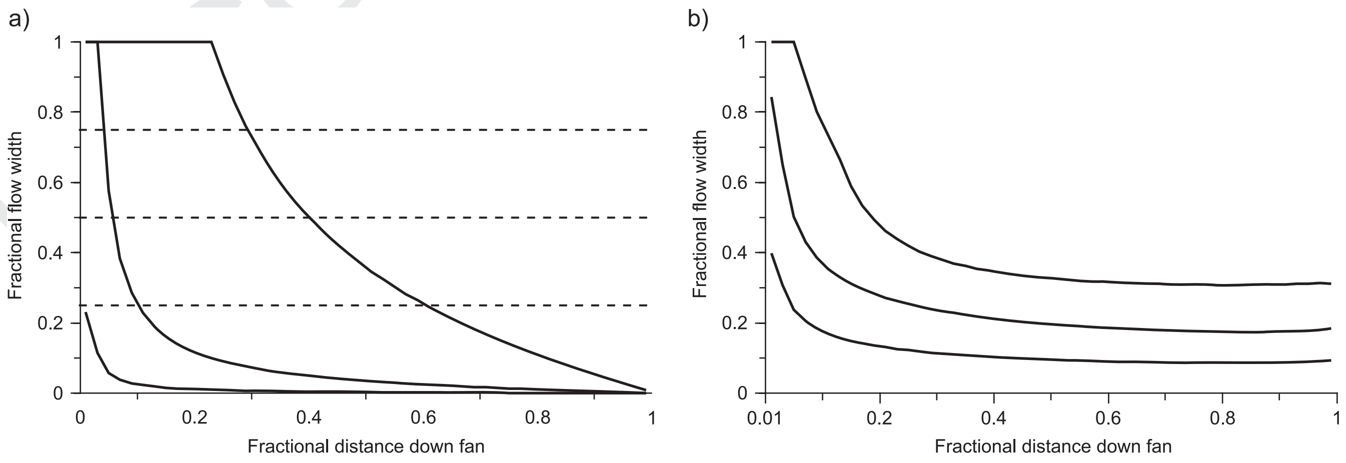

Figure 3. Relationships between fractional flow width (flow width divided by fan width) and fractional distance downfan (distance divided by fan length) for a range of simple theoretical models. (a) Dashed and solid lines represent, respectively, the expanding sheetflow model and channelized flow model of Parker *et al*. (1998). Channelized flow solutions are shown for fan aggradation rates that increase from bottom to top by two-orders of magnitude (i.e. in relative terms these solutions represent aggradation rates of 1, 10 and 100). (b) Relationships derived using Equations 1 to 5 presented in this article. Solutions are shown for discharges that increase from bottom to top (in relative terms these solutions represent water discharges of 1, 4 and 16).

DOI: 10.1002/esp

Nicholas and Quine (2007) present an alternative model for representing (predicting) flow width on alluvial fans, motivated by the need to examine non-equilibrium conditions, and so to represent spatial and temporal transitions between sheetflow and channelized flow configurations. This model defines separate widths for the cases of channelized flow and sheetflow and calculates the rate of sediment transport under each flow regime. It also determines the fraction of time spent in sheetflow and channelized states (see later), based on which a time-averaged sediment transport rate is determined (as the weighted sum of channelized and sheetflow transport rates). A single effective (time-averaged) flow width is then determined as that required to transport sediment at the time-averaged rate.

In order to implement this approach a single equation is used to determine the width of both channelized flow and sheetflow for conditions of known (given) effective (dominant) discharge (Q, in $m^3 s^{-1}$), sediment supply rate (Qs, in $m^3 s^{-1}$) and sediment calibre (D, in metres). Combining the mass continuity equation with a Manning–Strickler resistance law yields Equation 1:

$$Q = \int_0^W K_1 S^{1/2} D^{-1/6} h(y)^{5/3} dy \tag{1}$$

where K_1 is a constant with a value of approximately 10–25 ($m^{0.5} s^{-1}$), S is downfan gradient and h is flow depth (in metres), which varies as a function of lateral distance across the fan (y, in metres). To predict flow width (W, in metres) using Equation 1 it is necessary to define the flow depth distribution across the fan. This is achieved using the statistical model of Ferguson (2003), which itself must be constrained by the mean flow depth and a measure of flow variability. Although this assumption might be relaxed in future, here we assume that both channelized and sheetflow states are characterized by the same degree of flow variability (defined using the parameterization given by Ferguson for alluvial channels). In the case of channelized flow we implement Parker's (1978) hypothesis to constrain the mean flow depth ($\bar{h}$) as a simple multiple of the fan sediment size (D) and gradient (S)

$$\bar{h} = K_2 D/S \tag{2}$$

where K_2 is a dimensionless constant that takes a value between approximately 0·1 and 0·5 depending upon the value taken for the critical dimensionless shear stress and on the degree of bank cohesion.

In the case of sheetflow we hypothesize that mean flow depth when the fan is just fully inundated ($\overline{h_{IN}}$) is set by the height of low-relief bedforms that are characteristic of fan aggradation under non-channelized flows (Blair and McPherson, 1994; Whipple *et al.*, 1998). Data from alluvial fans in the Avoca Valley, New Zealand suggest that this height is a linear function of surface sediment size

$$\overline{h_{IN}} = K_3 D \tag{3}$$

where K_3 is a dimensionless constant that takes values of approximately 4–10. Widths are further constrained by noting that flow width must be equal to or less than fan width, and channelized flow width must be equal to or less than sheetflow width.

Having determined flow width for both channelized and sheetflow states, the total volumetric sediment transport rate for each state is determined using a Meyer-Peter and Muller type relation:

$$Q_S = \int_0^W K_4 D^{3/2} \left[\tau(y)^* - \tau_C^* \right]^{1.5} dy \tag{4}$$

where K_4 is a constant with a value of approximately 10–100 ($m^{0.5} s^{-1}$), τ^* is the dimensionless shear stress (related to the flow depth by applying a normal flow approximation) and τ^*_C is the critical dimensionless shear stress at which sediment is entrained. Equation 4 is applied separately to channelized and sheetflow states, and a time-averaged sediment transport rate is then derived by weighting each transport rate by the fractional time spent in the corresponding state. Nicholas and Quine (2007) proposed that these times are a function of the rate of fan aggradation (for constructional fans). They represent this effect by expressing the proportion of time (P) spent in a channelized state as:

$$P = e^{-\phi T/A} \tag{5}$$

where A is the cross-sectional area of the flow in a channelized state, T is a characteristic time scale (in seconds) that is related to the periodicity of cut-fill cycles, and ϕ is the areal rate of aggradation (in $m^2 s^{-1}$) at the point down the fan in question (averaged over time period T).

Application of Equations 1 to 5 allows the time-averaged sediment transport rate (Qs) to be calculated for given values of Q, D, S, K_1, K_2, K_3, K_4 and T. Where Qs is known but S is unknown this approach can be implemented iteratively to determine the fan slope required to convey a given sediment supply rate. By applying these equations at a series of points down the fan the average shape of the fan radial profile can be determined. Typical relationships between fractional flow width and distance down fan for this model are shown in Figure 3(b). Comparison of this model with the expanding sheetflow and channelized flow models of Parker *et al.* (1998) yields two important observations. First, the patterns of fractional flow width shown in Figure 3(b) are indicative of a transition from channel-dominated flow on the upper portions of the fan to sheetflow-dominated conditions at the fan toe (compare with separate trends for sheetflow and channelized flow in Figure 3a). This transition is a product of the downfan increase in areal fan aggradation rate (A) that results from the increase in fan width (assuming a spatially-uniform rate of vertical aggradation). Second, flow width modelled using Equations 1 to 5 is strongly dependent on discharge, whereas in the channelized flow model of Parker *et al.* (1998) width is dependent upon sediment transport rate and independent of discharge. The strong dependence of width on sediment transport rate in the Parker channelized flow model results from the assumption of constant dimensionless Shields stress, which sets the unit sediment transport rate and thus determines the flow width needed to convey a given sediment load. In this model, changes in imposed discharge are accommodated by changes in equilibrium slope rather than flow width. In contrast, the sheetflow component of the model of Nicholas and Quine (2007) incorporates a simple relationship linking flow width to flow depth (Equation 3), such that flow width is dependent upon both sediment load and discharge.

Experimental Setup

This study aims to test the simple theoretical model presented earlier using data from an experimental investigation of changes in the width and configuration of flow during alluvial fan construction. Experimental work was conducted at the University of Exeter Sediment Research Facility in a custom built alluvial fan simulation basin. This consists of a three metre square

DOI: 10.1002/esp

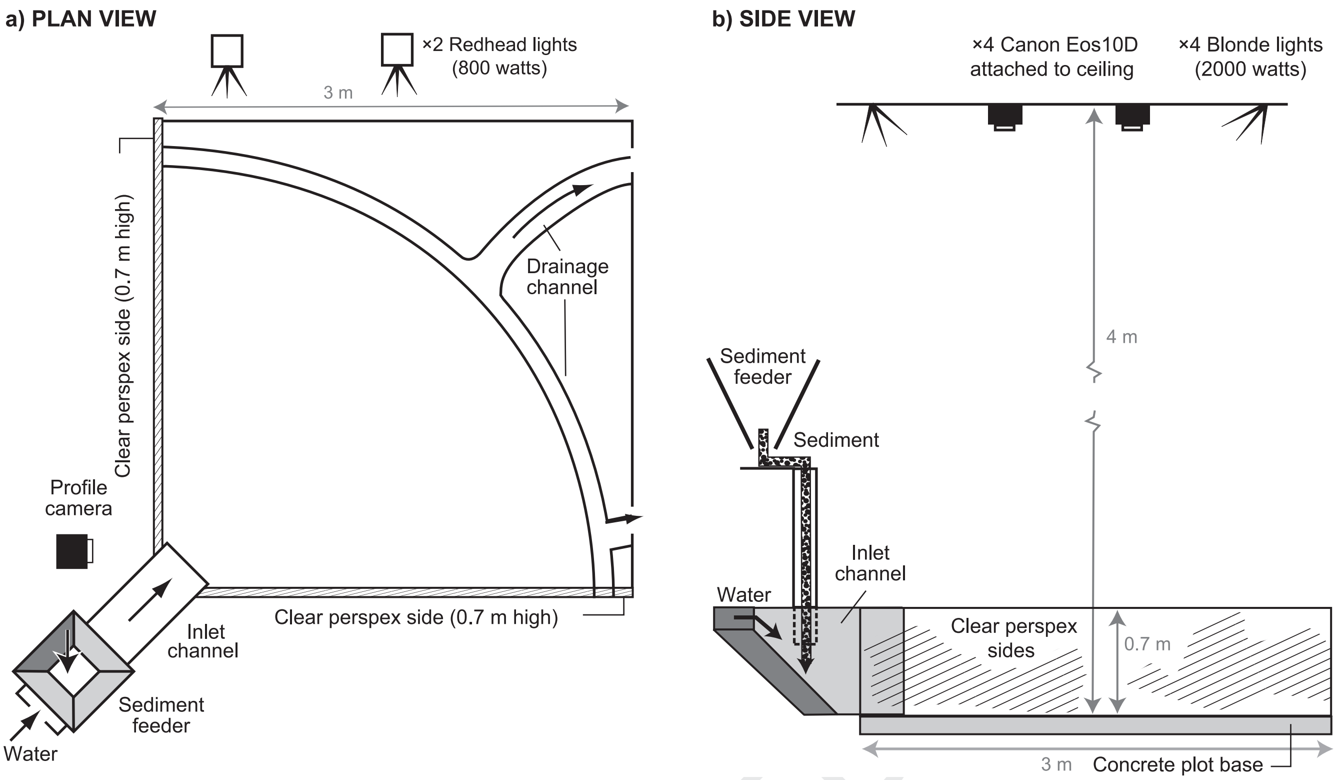

Figure 4. Experimental set-up used for physical modelling of fan evolution.

basin with controlled sediment and water supply fed through an inlet channel to the fan apex (see Figure 4). A variable speed gravity-fed sediment hopper supplies the sediment at a constant rate (25 g s^{-1}) to the inlet channel where it mixes with the water, being fed at a constant discharge (0·1 l s^{-1}) from a regulated pressure tank, before reaching the entrance to the basin. The sediment used in this experiment was a unimodal sand with particle sizes in the range 0·15 mm to 1·0 mm and a median diameter of 0·6 mm. The fan area is enclosed on two sides by clear Perspex 0·7 metres high, with an opening at the apex where the inlet channel is positioned, restricting the angle of the fan to 90º. The surface of the basin is constructed from concrete with a curved drainage channel cut into it to assist the removal of water and sediment from the basin once the fan reaches its maximum extent. At the start of the experiment the basin is empty and as the experiment proceeds a fan develops at the apex and progrades across the basin until it reaches the drainage channel. Continuous flushing of this channel prevents further growth of the fan. Near-continuous patterns of evolving fan morphology and flow characteristics were recorded using an array of four overhead digital SLR cameras taking photographs of the basin surface at a temporal resolution of *c.* 10 minutes. Adequate illumination of the experimental basin was provided by specialist stage lighting. Potassium permanganate was used as a dye, added to the water shortly before each photograph was taken, to assist with the identification of wet and dry areas of the fan. Photographs were analysed using ERDAS Imagine Spatial Modeller to derive binary wet/dry images. Wet regions were extracted using values of the ratio of red to green image bands (to remove the influence of variable illumination on the experimental basin). Threshold ratio values were determined separated for each photograph and wet/dry images were then checked independently to ensure that areas had not been misclassified. For each image, individual wet pixels were binned into classes at intervals down the fan in order to calculate the mean fractional flow width as a function of downfan distance. Although the results presented in this article relate to a single experimental setup, subsequent experiments confirm that the spatial and temporal changes in flow width and configuration during fan construction reported in this article are characteristic of a wide range of water and sediment feed rates (Clarke, 2009).

Results

Figure 5 shows the change in the mean fan length and vertical rate of aggradation on the fan over the duration of the laboratory experiment (*c.* 700 minutes). Progradation of the fan from the basin inlet was associated with a progressive increase in fan area and length over the first 500 minutes of the experiment, but at a rate that declined through time. Changes in fan extent after *c.* 500 minutes were apparent although minor. Flushing of sediment from the drainage channel became necessary after *c.* 370 minutes, indicating that before this time 100% of sediment fed to the basin went into storage on the fan. After

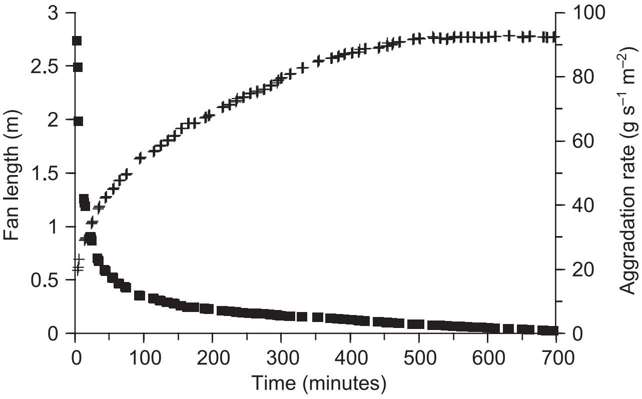

Figure 5. Changes in mean fan length (pluses) and fan aggradation rate (squares) over the course of the laboratory experiment.

DOI: 10.1002/esp

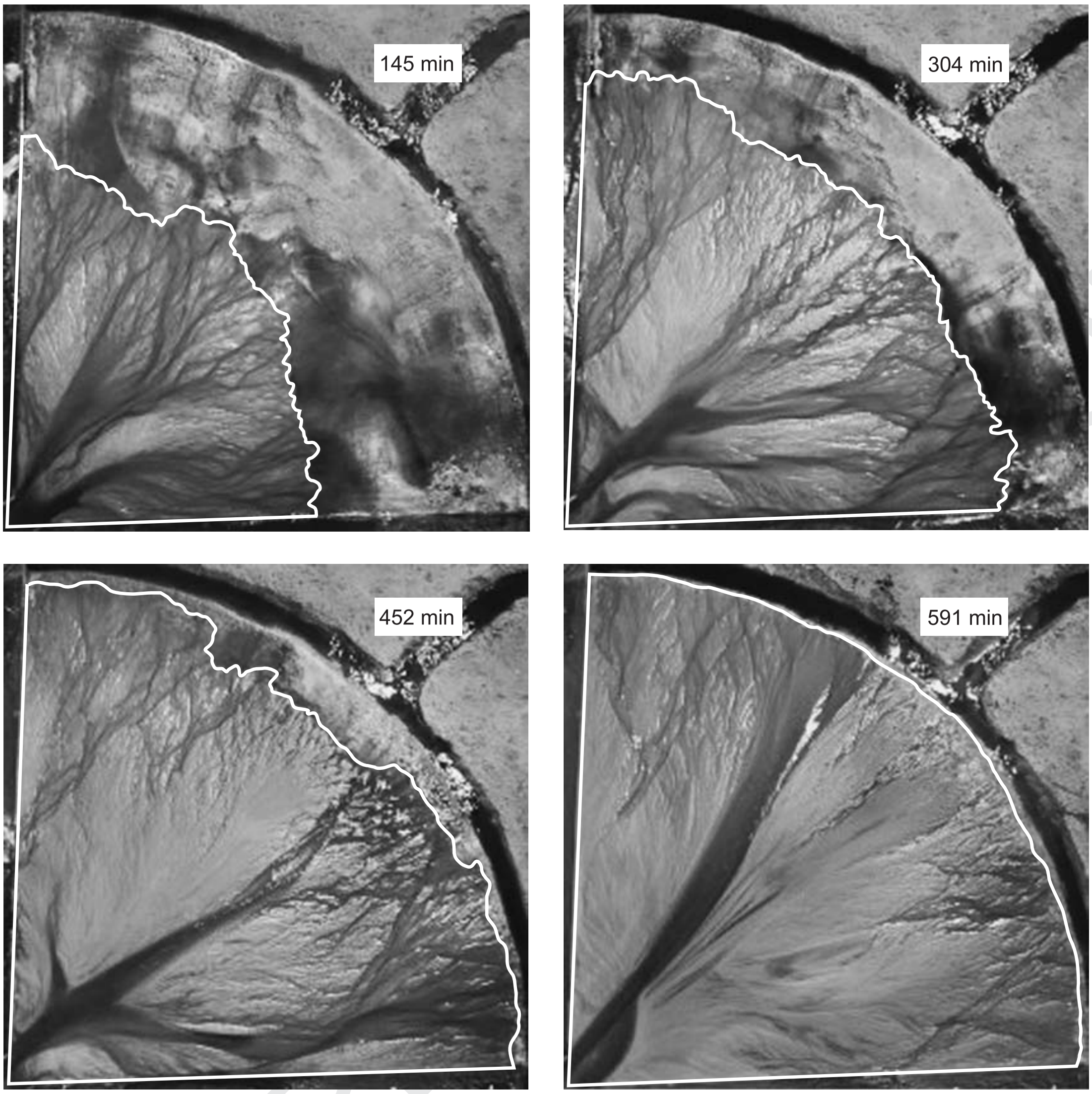

Figure 6. Photographs showing temporal changes in fan size and flow configuration at four points in time during the laboratory experiment.

700 minutes, the majority of sediment supplied to the basin was transported off the fan, indicating that the fan had stabilized. The mean vertical aggradation rate on the fan declined through time (see Figure 5) as a result of the progressive increase in fan area. In the absence of continuous measurements of the volume of sediment flushed from the drainage channel, aggradation rates shown in Figure 5 for the period after 370 minutes have been estimated by assuming a linear decline though time in the fraction of sediment going into storage on the fan between 370 and 700 minutes. This assumption has a limited influence on the trend shown in Figure 5 because the bulk of the reduction in aggradation rate over the course of the experiment is associated with the increase in fan area.

Spatial and temporal patterns of fan building and flow configuration were complex, with the number of channels and their geometry adjusting continuously while the fan developed (see Figure 6). Sediment deposition was associated with both sheetflow and with channel formation, migration and abandonment. Channels were observed to form on all parts of the fan throughout the course of the experiment, although as in previous studies, the deepest flows occurred at the fan apex (Schumm *et al.*, 1987; Whipple *et al.*, 1998). In the earliest stages of the experiment sheetflow dominated the fan, with over half the fan surface covered with water and no clear channels being present. As the fan prograded, the flow alternated between sheetflow and channelized states, with the latter being typically both unstable and braided. Similarly, after the initial stages of the experiment, continuous regions of water (termed here sheetflow) were characterized by small-scale variability in flow depth, giving the appearance of intricate braided networks. As the experiment progressed, channels became more pronounced and typically reduced in number until, after *c.* 600 minutes, the fan became dominated by a single channel. This channel became entrenched at the apex, and was periodically associated with terrace formation in the upper fan, although it continued to avulse and migrate in the mid and lower fan regions. During the latter stages of the experiment, the rate of movement of this channel declined and sediment deposition was limited to the fan toe.

Figure 7 shows spatial patterns of fractional flow width for two windows in time over the course of the experiment (60–80 minutes and 570–590 minutes). Although flow configurations were highly variable in time and space, the patterns evident in these diagrams are indicative of the broad trends over the duration of the experiment. During the early stages of fan progradation, flow width was typically greater and more temporally-variable (fractional widths varied between 0·3 and 1 over periods of a few minutes). As the experiment progressed, flow widths typically declined and, although remaining highly temporally-variable, the time period between major reorganizations of flow pathways (and hence changes in flow width) tended to increase. Throughout the course of the experiment,

DOI: 10.1002/esp

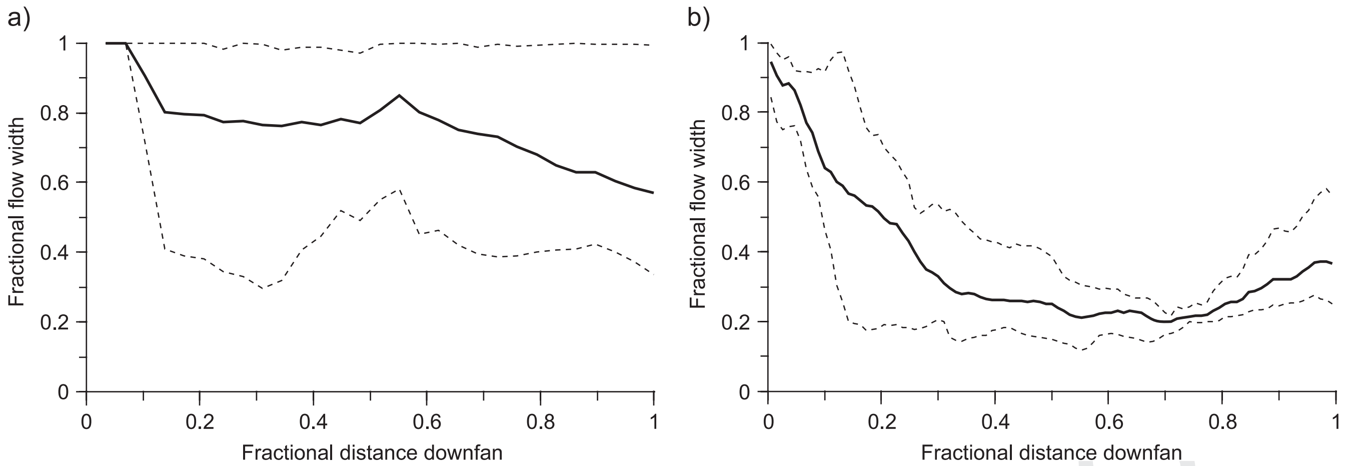

Figure 7. Relationships between fractional flow width and fractional distance downfan for two time periods during the laboratory experiment: (a) 60–80 minutes; (b) 570–590 minutes. Solid lines represent the mean flow width derived from three wet/dry images obtained during each period. Dashed lines represent the maximum and minimum flow widths derived from these images.

patterns of fractional flow width were often characterized by two distinct regions on the fan: an upper region in which fractional widths declined sharply in a downfan direction, and a lower region of relatively uniform fractional widths. After *c.* 250 minutes this lower region was also frequently characterized by a small increase in fractional widths at the toe of the fan. Periodically, the upper portion of the fan was inundated by sheetflow and the region of sharply declining fraction widths advanced down the fan, before subsequently retreating as channelized flow was re-established.

Direct comparison between the experimental data and theoretical model is problematic because, while the experimental data provide information about instantaneous patterns of flow width, the model simulates the time-averaged width on the fan. As a result, experimental data reflect short-term fluctuations between channelized and sheetflow states that are parameterized (and hence not represented explicitly) by Equation 5. Furthermore, the model presented earlier includes a number of parameters that cannot be measured and must instead by calibrated against the experimental data. Consequently, rather than attempting to make direct comparisons with the observed fractional flow widths, we focus here on the potential for the model to reproduce the key trends in spatial and temporal patterns of fractional flow width that are apparent in the experimental data. To do this we apply the model to predict the spatial patterns of fractional flow width on the fan for the known water and sediment supply rates and the calculated rates of fan aggradation and mean fan length (Figure 5). We use a parameter set that is physically plausible (K_1 = 15, K_2 = 0·3, K_3 = 4, K_4 = 75, T = 0·1 hours) and which yields width predictions that are consistent with the experimental data. Furthermore, these parameters yield a mean predicted fan slope of *c.* 0·09 once the fan reaches its maximum extent, which is consistent with the observed mean slope of *c.* 0·089. It should also be noted that while the choice of parameter values influences the width predictions in absolute terms, the relative downfan patterns of fractional width and their temporal evolution over the course of the experiment are largely independent of the choice of parameter values. Furthermore, implementation of the model using an alternative formulation of Equation 1 based on a Chezy resistance law yielded spatial and temporal patterns of fractional flow width consistent with those reported here. In this sense the model output presented here should be considered robust.

Figure 8 shows patterns of modelled fractional flow width at eight points in time during the experiment. These patterns

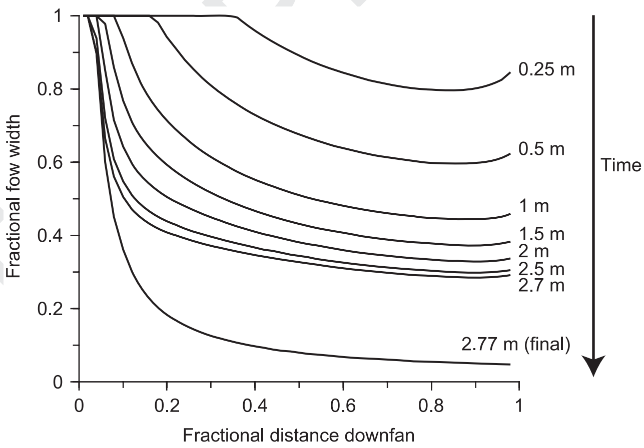

Figure 8. Modelled relationships between fractional flow width and fractional distance downfan at eight points in time over the course of the laboratory experiment. Labels indicate the fan extent at each point in time. The relationship labelled 'final' represents the modelled flow width when the fan has ceased to aggrade.

share many of the characteristics that are evident in the experimental data. For example, fractional widths decline sharply with distance downfan in the upper region of the fan and are relatively uniform in the lower region. Furthermore, fractional widths undergo a significant reduction over the course of the experiment as the rate of aggradation on the fan declines. There is also a marked reduction in flow width between the time that the fan approaches its maximum extent (*c.* 2·77 m) and when sediment accumulation on the fan ceases completely (marked 'final' on Figure 8). Although these patterns have been generated for a particular set of model parameter values, the spatial and temporal trends in fractional flow width described earlier are consistent with a much wider range of parameter values.

In order to make a more direct comparison of the modelled and observed relationships between aggradation rate and fractional flow width, experimental data and model results were used to calculate the mean rate of change of flow width over the course of the experiment. In the case of the experimental data, this was achieved by fitting a linear relationship to the fractional flow width time series at each point down the experimental basin. The gradient of these relationships indicates the mean rate of flow width narrowing over the experiment. For both model output and experimental data these

DOI: 10.1002/esp

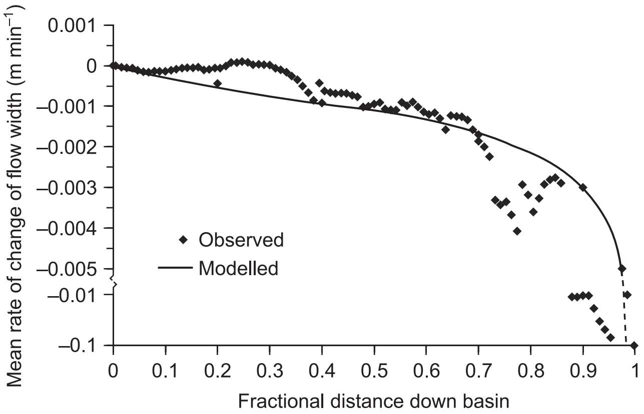

Figure 9. Modelled and observed relationships between the temporal rate of change of flow width and fractional distance down the experimental basin.

relationships were determined over the time period between the point at which the fan prograded to that part of the basin and the end of the experiment. Modelled and observed relationships are consistent with one another (see Figure 9) and are indicative of a progressive increase in the rate of flow narrowing with distance down the experimental basin. This trend reflects both the greater reduction in absolute flow width towards the end of the basin and the shorter time period over which narrowing of the flow occurs. The former is a product of the tendency for flow width to increase towards the lower end of the fan during the period of fan construction, which is itself a result of the downfan increase in areal aggradation rate.

Discussion

The results outlined earlier demonstrate that the theoretical model presented here captures both the key spatial and temporal trends in observed time-averaged flow width during the experiment. Furthermore, these trends can be explained in terms of spatial and temporal changes in aggradation rate during fan construction and stabilization, thus highlighting the significance of non-equilibrium conditions as a control on flow width and indicating that models based on equilibrium concepts may have important limitations in such situations. Despite this observation, comparison of the results obtained using Equations 1 to 5 with those of previous models of flow width on alluvial fans indicates that, in some respects, these alternative models produce consistent results. For example, under conditions of spatially-uniform vertical aggradation rate, Equation 5 dictates that the associated downfan increase in areal aggradation rate will promote a transition from channelized flow to sheetflow conditions. The resulting fractional flow width curves (Figures 3b and 8) are consistent with a transition from the channelized flow model of Parker *et al*. (1998) in the upper portion of the fan to the expanding sheetflow model at the fan toe (e.g. in Figure 3a). In contrast, predicted changes in flow width resulting from a reduction in fan aggradation rate (associated with an increase in fan length under conditions of constant sediment supply) differ significantly between equilibrium and non-equilibrium models. For example, Figure 9 illustrates that for any location within the experimental basin, the non-equilibrium model presented in this article predicts that flow width declines through time (because declining vertical aggradation rates reduce the fraction of time spent in a sheetflow state). In contrast, under conditions of constant sediment supply and spatially-uniform, but temporally-declining, vertical aggradation rate (e.g. due to increasing fan length) the channelized flow model of Parker *et al*. (1998) predicts that flow width at any point within the basin will increase as the fan lengthens. This occurs because flow width is proportional to sediment transport rate in this model, and the total sediment transport rate at any fixed distance from the fan apex increases as the fan lengthens. Comparisons with the expanding flow model of Parker *et al*. (1998) are not possible because it does not relate the fractional flow width to the physical characteristics of the system.

As noted previously, although the absolute flow widths derived using Equations 1 to 5 are dependent on a number of parameter values, the spatial and temporal trends described earlier are unchanged across a wide range of parameterizations. Of these parameters, it is the characteristic time-scale (T) in Equation 5 that is central to the representation of the relationship between aggradation rate and the transition between sheetflow and channelized flow conditions. Figure 10(a) illustrates the sensitivity of predicted flow widths to variations in T. As would be expected, an increase in T leads to a larger fraction of time spent in a sheetflow state and thus an increase in time-averaged fractional flow width. Logic dictates that this parameter should scale with the periodicty of cut-fill cycles or the average life-time of individual channels, hence for the current experimental setup T is on the order of minutes to

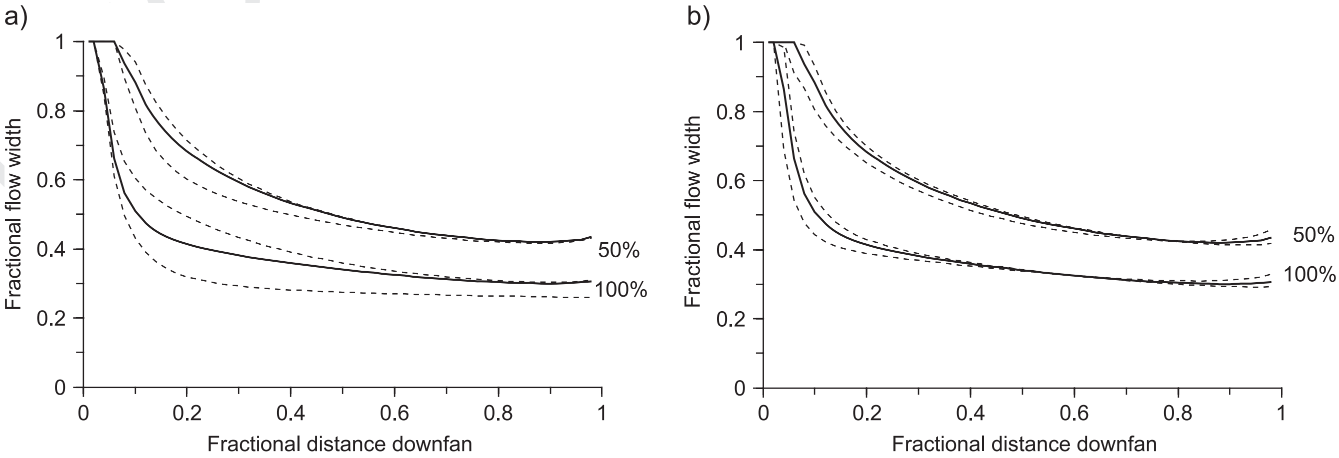

Figure 10. Modelled relationships between fractional flow width and fractional distance downfan for fans with lengths equal to 50% and 100% of their maximum extent during the experiment. Results are shown for: (a) three values of the characteristic time-scale (T): T = 0·05 hours (lower, dashed curves), T = 0·1 hours (middle, bold curves), and T = 0·2 hours (upper, dashed curves); (b) three values of Ferguson's flow variability index (b): b = 0·3 (upper, dashed curves), b = 0·55 (middle, bold curves), and b = 0·8 hours (lower, dashed curves).

DOI: 10.1002/esp

tens of minutes. However, on this basis one might also expect *T* to vary through time as the fan progrades and stabilizes (and possibly with distance down the fan). Furthermore, *T* may itself be a function of fan aggradation rate. While the current use of a constant value of *T* has the advantage of simplicity, the physical basis of the parameterization provided by Equation 5 and the potential for applying this to a wider range of boundary conditions without the need for arbitrary calilbration may be improved by attempting a more precise and physically-based definition of *T*.

Sediment transport rates on the fan, and hence flow widths, are also likely to be sensistive to variability in flow depth and shear stress, represented here by integrating sediment transport calculations over a stress distribution defined using the approach of Ferguson (2003). We adopt a distribution consistent with observations made in alluvial channels ($b = 0{\cdot}55$, see Ferguson 2003: p. 6) and apply this measure of flow variability uniformly in space and time. Consequently, this approach does not account for differences in flow variability between sheetflow and channelized flow conditions. We incorporate flow variability in our model because it reduces model sensitivity to variations in mean flow depth close to the threshold of sediment motion. Differences in flow variability between sheetflow and channelized flow are neglected here because we lack the data needed to parameterize these relationships reliably. As with other parameters, altering the value of *b* used to represent flow variability will alter the absolute values of modelled flow widths, fan slopes and sediment transport rates (increasing flow variability has the same effect as increasing the value of K_4). However, altering *b* has little or no influence on the relative downfan patterns of fractional width and their temporal evolution over the course of the experiment (see Figure 10b), because it is assigned a value that is uniform in space and time. In order to evaluate the scope for improving the physical basis of model representations of both flow variability (*b*) and cut-fill periodicity (*T*) we are currently carrying out time-series analysis of flow width data obtained for a series of experiments conducted for varying water and sediment supply conditions.

Summary

Autogenic feedbacks between geomorphic processes and landforms have the potential to promote complex behaviour during landscape evolution. However, at present we are ill-equipped to interpret the evidence for such behaviour in the past, or predict its occurrence in the future, due to our limited understanding of process-form interactions under non-equilibrium conditions. This article has addressed this issue for the particular case of alluvial fan construction, by presenting results from an experimental study of spatial and temporal changes in flow width and configuration during fan progradation and stabilization. Comparison of experimental data with a new model of flow width under non-equilibrium conditions demonstrates that the model captures the observed spatial and temporal patterns of time-averaged flow width adjustment on the fan, and that these trends can be explained in terms of spatial and temporal changes in rates of vertical aggradation and fan geometry. Comparison of the non-equilibrium width model with existing models of flow width for fans experiencing equilibrium aggradation illustrates that the new approach provides an improved capability to represent spatial patterns of flow width associated with a transition from channelized to sheetflow states. Perhaps more significantly, temporal patterns of flow width adjustment predicted by the new approach (associated with increasing fan length during progradation) are consistent with experimental observations, and the reverse of those derived by applying a channelized flow approximation alone. These results have implications for modelling fluvial environments more generally, and suggest that alluvial flow width models derived for equilibrium conditions may have limited utility in non-equilibrium situations, despite their widespread use to date.

Acknowledgements—This work was funded by a Natural Environment Research Council grant NER/B/2002/00357 and by an Exeter University PhD Scholarship to Lucy Clarke. We are grateful to Rob Ferguson and one anonymous reviewer whose perceptive comments led to improvements in the manuscript.

References

Blair TC, McPherson JG. 1994. Alluvial fans and their natural distinction from rivers based on morphology, hydraulic processes, sedimentary processes, and facies assemblages. *Journal of Sedimentary Research* **A64**: 450–489.

Church M, Ryder JM. 1972. Paraglacial sedimentation; a consideration of fluvial processes conditioned by glaciation. *Geological Society of America Bulletin* **83**: 3059–3072.

Clarke L. 2009. *Alluvial Fan Dynamics: An Experimental Investigation*, unpublished PhD Thesis, University of Exeter, 298 pp.

Clevis Q, De Boer P, Wachter M. 2003. Numerical modelling of drainage basin evolution and three-dimensional alluvial fan stratigraphy. *Sedimentary Geology* **163**: 85–110.

Coulthard TJ, Macklin MG, Kirkby MJ. 2002. A cellular model of Holocene upland river basin and alluvial fan evolution. *Earth Surface Processes and Landforms* **27**: 269–288.

Ferguson RI. 2003. The missing dimension: effects of lateral variation on 1-D calculations of fluvial bedload transport. *Geomorphology* **56**: 1–14. DOI: 10.1016/S0169-555X(03)00042-4

Francis RA. 2006. Allogenic and autogenic influences upon riparian vegetation dynamics. *Area* **38**: 453–464. DOI: 10.1111/j.1475-4762.2006 .00706.x

Hartley AJ, Mather AE, Jolly E, Turner P. 2005. Climatic controls on alluvial fan activity, Coastal Cordillera, northern Chile. *Geological Society: London: Special Publications* **251**: 95–116.

Harvey AM. 2002a. Effective timescales of coupling in fluvial systems. *Geomorphology* **44**: 175–201.

Harvey AM. 2002b. The role of base-level change in the dissection of alluvial fans: case studies from southeast Spain and Nevada. *Geomorphology* **45**: 67–87. DOI: 10.1016/S0169-555X(01)00190-8

Harvey AM. 2005. Differential effects of base-level tectonic setting and climatic change on Quaternary alluvial fans in the northern Great Basin, Nevada, USA. *Geological Society: London: Special Publications* **251**: 117–131.

Hooke R, Dorn RI. 1992. Segmentation of alluvial fans in Death Valley, California: new insights from surface exposure dating and laboratory modelling. *Earth Surface Processes and Landforms* **17**: 557–574.

Humphrey NF, Heller PL. 1995. Natural oscillations in coupled geomorphic systems: an alternative origin for cyclic sedimentation. *Geology* **23**: 499–502.

Kim W, Jerolmack DJ. 2008. The pulse of calm fan deltas. *Journal of Geology* **116**: 315–330. DOI: 10.1086/588830

Kim W, Muto T. 2007. Autogenic response of alluvial-bedrock transition to base-level variation: experiment and theory. *Journal of Geophysical Research* **112**: F03S14. DOI: 10.1029/2006JF000561

Muto T, Swenson JB. 2006. Autogenic attainment of large-scale alluvial grade with steady sea-level fall: an analog tank-flume experiment. *Geology* **34**: 161–164.

Nicholas AP, Quine TA. 2007. Modelling alluvial landform change in the absence of external environmental forcing. *Geology* **35**: 527–530.

Parker G. 1978. Self-formed straight rivers with equilibrium banks and mobile bed. Part 2. The gravel river. *Journal of Fluid Mechanics* **89**: 127–146. DOI: 10.1017/S0022112078002505

Parker G, Paola C, Whipple KX, Mohrig DC. 1998. Alluvial fans formed by channelised fluvial and sheet flow, I, theory. *Journal of*

Hydraulic Engineering **124**: 985–995. DOI: 10.1061/(ASCE)0733-9429(1998)124:10(985)

Ritter JB, Miller JR, Enzel Y, Wells SG. 1995. Reconciling the roles of tectonism and climate in Quaternary alluvial fan evolution. *Geology* **23**: 245–248. DOI: 10.1130/0091-7613(1995)023<0245:RTROTA>2.3.CO;2

Schumm SA, Parker RS. 1973. Implications of complex response of drainage systems for Quaternary alluvial stratigraphy. *Nature* **243**: 99–100.

Schumm SA, Mosley MP, Weaver WE. 1987. *Experimental Fluvial Geomorphology*. John Wiley and Sons: New York; 413 pp.

Stouthamer E, Berendsen HJA. 2007. Avulsion: the relative roles of autogenic and allogenic processes. *Sedimentary Geology* **198**: 309–325. DOI: 10.1016/j.sedgeo.2007.01.017

Viseras C, Calvache ML, Soria JM, Fernández J. 2003. Differential features of alluvial fans controlled by tectonic or eustatic accommodation space. *Geomorphology* **50**: 181–202. DOI: 10.1016/S0169-555X(02)00214-3

Whipple KX, Trayler CR. 1996. Tectonic control on fan size: the importance of spatially variable subsidence rates. *Basin Research* **8**: 351–366.

Whipple KX, Parker G, Paola C, Mohrig DC. 1998. Channel dynamics, sediment transport and the slope of alluvial fans: experimental study. *Journal of Geology* **106**: 677–693.